PHYSICAL REVIEW C

NUCLEAR PHYSICS

THIRD SERIES, VOLUME 32, NUMBER 6 DECEMBER 1985

Coulomb energy systematics and the missing $J^\pi = \frac{1}{2}^+$ state in ^{9}B

R. Sherr
Department of Physics, Princeton University, Princeton, New Jersey 08544

G. Bertsch*
Department of Physics, University of Tennessee, Knoxville, Tennessee 37996

(Received 22 July 1985)

We study the energy systematics in light mirror nuclei of the unbound states having predominant single-particle character. For many levels in the mass range $A=9$–17, the observed Thomas-Ehrmann shift is described very well by a simple potential model. We speculate that the missing partner in ^{9}B of the $\frac{1}{2}^+$ state in ^{9}Be is observable as a broad continuum with a peak at 0.9 MeV.

I. INTRODUCTION

Many experiments have been carried out in the past 25 years to look for the analog in ^{9}B of the 1.685 MeV, $J=\frac{1}{2}^+$ state in ^{9}Be. The first excited state in ^{9}B has been reported at various locations between 1.2 to 1.7 MeV, and it has occasionally been presumed to be that analog. A state is listed in the most recent compilation[1] by Ajzenberg-Selove at (1.6) MeV with a width of 700 keV, but no J^π assignment is given.

The search for low-lying states in ^{9}B is made very difficult because all states are particle unbound. The ground state and the $\frac{5}{2}^-$ deformed state at 2.36 MeV have small widths, but all other $T=\frac{1}{2}$ levels have widths greater than 400 keV. The situation is similar for ^{9}Be which, except for the ground state, has only particle unbound states. The first excited state of ^{9}Be, with $J^\pi=\frac{1}{2}^+$ at 1.685 MeV excitation, has a width of 150 keV and is unbound by 20 keV. Because this is a single-particle state in s-wave scattering the resonance does not have the usual Breit-Wigner line shape, but is very skewed.[2]

Bauer *et al.*[3] have reviewed the experimental evidence for a broad state near 1.5 MeV in the reactions ^{6}Li(α,n), ^{9}Be(p,n), and ^{12}C(p,α). They conclude that decays into three- and four-body final states obscure the 1.5 MeV region for a possible weakly excited level. Similar problems[4–6] arise in other reactions such as ^{10}B(p,d), ^{10}B(^{3}He,^{4}He), and ^{7}Li(^{3}He,n).

The charge exchange reaction has also been used to investigate the low-lying spectrum of ^{9}Be. Ueno *et al.*[7] studied the reaction ^{9}Be(^{3}He,t) at bombarding energies between 5.5 and 7.8 MeV, and did not find a resonance near 1.6 MeV. Instead, they found a relatively strong broad continuum starting at the ground state and reaching a maximum below 2 MeV of excitation. The yield is quite forward peaked, and the maximum moves to higher energy as the bombarding energy is increased. The continuum was well fitted by a description in which four-body phase space ($\alpha+\alpha+$t+p) was multiplied by a Coulomb penetrability factor for the triton and the mass 9 system. Recent measurements of the (^{3}He,t) reaction at 90 MeV (Ref. 8) also show no sharp features at 1.6 MeV. However, in this work, the continuum is interpreted as a broad state ($\Gamma=1.0\pm0.2$ MeV) at 1.65 ± 0.03 MeV excitation, and is presumed by the authors to be the analog of the 1.68 MeV, $J=\frac{1}{2}^+$ state of ^{9}Be.

We shall question here whether the analog of a $\frac{1}{2}^+$ state in ^{9}Be at 1.68 MeV could be at about the same excitation in ^{9}B. The main point is that if it were a single-particle $2s_{1/2}$ state, one would expect its excitation energy to be considerably lowered by the Thomas-Ehrman effect.[11] The possibility of a lower energy for the state was raised in Ref. 7, and also by Barker and Treacy[9] who fitted a (^{3}He,α) spectrum[10] with a density-of-states function for an s wave state at $E=1.2$ MeV and a width of 1.0 MeV. However, this reaction is not favorable because of the low $2s_{1/2}$ probability in the ^{10}B ground state wave function.

In this paper, we calculate the location and shape of the $\frac{1}{2}^+$ level in ^{9}B, using a single-particle potential model. Our intention is to guide future experiments by providing estimates of the position, width, and line shape of the state. In the course of this study, we found that our computations covering a range of light nuclei gave a satisfactory overall description of the widths and Coulomb shifts of single-particle states. Since it is more complete than previous studies, we will present our calculations for these other nuclei as well.

The first comprehensive study of Coulomb displacement energies of analog states with potential models was by Nolen and Schiffer.[11] They used a Woods-Saxon potential, constraining the radius and depth to reproduce the empirical neutron binding energies. They determined the radius of the Coulomb potential from the measured charge distributions of the closed shell cores. Their computed displacement energies were always smaller than the experimental values (by 4% to 9%). Numerous correction terms failed to remove this anomaly. On the easier question of the relative energy shifts of excited states, they found very good results for the $2s_{1/2}$ states in $A=13$ and 17.

A simpler approach was used in earlier papers by Nolen, Schiffer, and their collaborators.[12,13] Instead of demanding that the Coulomb potential fit the known charge distribution, it was only required that the ground state Coulomb energy be reproduced. In a study of the $\frac{7}{2}^-$ $(1f_{7/2})$ ground states of the odd Ca isotopes, they then predicted the Coulomb displacement energy for the $p_{3/2}$ excited states correctly (to within 26 keV). In another study, Schiffer[14] used Woods-Saxon potentials to calculate the widths of unbound proton states, finding reasonable agreement for the unbound orbits in ^{13}N and ^{41}Sc. Tombrello[15] had also made a study of Coulomb displacement energies using Woods-Saxon potentials of fixed radius.

II. CALCULATIONS AND COMPARISON WITH EXPERIMENTAL DATA

In the present investigation, we use the Woods-Saxon potential model in its simplest form (i.e., constant radius and diffuseness parameters) to compute excitation energies and widths of mirror states. Throughout our computations, we use the potential

$$V(r)=\frac{-V_0}{1+\exp(r-r_0A^{1/3})/a} \quad (1)$$

with parameters $r_0=1.25$ fm and $a=0.65$ fm. The well depth is usually chosen to fit the binding energy of the neutron (if bound) and the proton energy is then calculated for the same V_0, including a Coulomb field of a uniform spherical charge of radius $r_0A^{1/3}$. Unbound states appear as resonances. For some mirror pairs that are proton unbound, we fit V_0 to the proton level so that its width can be compared with experiment. As our goal is to predict the broad $s_{1/2}$ and $p_{1/2}$ resonances in ^{9}B, we shall be content with 100—200 keV accuracy in reproducing known energies in other nuclei.

A. $A=11$, 13, 15, and 17 mirrors

To test the simple potential model, we first carried out computations of mirror states for $A=11$, 13, 15, and 17. For $A=13$ and 17, the single-particle energies were calculated relative to the $(0^+,0)$ ground states of ^{12}C and ^{16}O. However, for $A=11$ and 15, the ground state spins of the ^{10}B and ^{14}N cores are nonzero, and, furthermore, stripping experiments and model calculations show that the lowest excited $\frac{1}{2}^-$, $\frac{1}{2}^+$, and $\frac{5}{2}^+$ states are predominantly single-particle levels relative to $(0^+,1)$ states of the cores. We therefore use binding energies relative to the $(0^+,1)$ excited level of ^{10}B or ^{14}N for $A=11$ or 15.

Our results for all the nuclei are summarized in Tables I and II. We first discuss the cases in which the states are bound or else well-defined resonances, deferring consideration of the broad states of $A=9$ until later. Table I lists the experimental and calculated values of excitation energies and level widths of only those states that have largely single-particle character. These excitation energies are also shown in the level diagrams of Figs. 1 and 2. The experimental widths in the references given usually correspond to FWHM; our computed widths are also FWHM values.

For $A=11$ and 15, all the states are bound, and the differences between calculated and experimental excitation energies are no larger than 100 keV for $A=11$ and 200 keV for $A=15$. The corresponding differences in Coulomb energies listed in Table II are at most 4% of the ground state Coulomb energy difference for $A=11$ and 10% for $A=15$. The agreement is better than should be expected, considering the doubtful assumption that the levels are pure single-particle states coupled to odd-odd 0^+ core configurations.

For $A=13$, the $\frac{1}{2}^+$ and $\frac{5}{2}^+$ proton states are unbound resonances. A resonance may be defined in principle as a pole in the scattering matrix, with the resonant energy being the real part of the pole's position. This definition is not easy to apply, so in practice, more convenient prescriptions are used for the resonant energy. One prescription, employed in Ref. 16, is to take the energy that maximizes an appropriately normalized wave function amplitude inside the nucleus. We apply this prescription by evaluating

$$\int_0^\infty \Psi_E^2(r)\frac{dV}{dr}r^2dr\ , \quad (2)$$

where $\Psi_E(r)$ is a continuum wave function for the single-particle state at energy E with respect to (core plus nucleon). It is normalized by

$$\Psi_E(r)\underset{r\to\infty}{\to}\frac{\sin(kr+\delta)}{\sqrt{kr}}\ . \quad (3)$$

The integral (2) provides a line shape for the excitation of a single-particle level by a surface-peaked reaction mechanism. The width of the level is taken to be the FWHM of (2). In Fig. 3(b), we show some results of this method by the curves labeled σ. Neither the energy nor the width will be the same as for Breit-Wigner fits of the elastic scattering resonance line shape, but for $\Gamma \ll E_b$, the differences will be negligible.

The same remarks hold for another practical definition[17,18] of the resonance, namely the energy at which the rate of increase of the nuclear phase shift is a maximum. Some results of this approach are illustrated by the curves labeled $d\delta/dE$ in Fig. 3(b). We shall discuss Fig. 3 in detail later on. For the present, we note that for the ^{13}C-^{13}N

TABLE I. Single particle states in mirror nuclei $A=9$ to 17. Experimental and computed excitation energies and the widths (FWHM) for unbound levels are listed for the $Z_<$ member of the pair in the fourth and fifth columns. Those for the $Z_>$ member are given in the sixth and seventh columns. The potential well depth V_0 is given in the eighth column, while the references for the experimental data are listed in the last column.

			$E_x^<$ (MeV)	$\Gamma^<$ (keV)	$E_x^>$ (MeV)	$\Gamma^>$ (keV)	V_0 (MeV)	Ref.
^{9}Be-^{9}B	$\frac{3}{2}^-$	expt.	0		0	0.5		1
		calc.	0.10		0	1.3	41.5	
	$\frac{1}{2}^+$	expt.	1.69	150	1.65	(~1000)		1,8
		calc.	1.70	230	0.93	1400	56.3	
	$\frac{1}{2}^-$	expt.	2.78	1080	(2.6)	(1650)		1,23
		calc.	2.80	~1300	2.40	~2400	28.4	
	$\frac{5}{2}^+$	expt.	3.05	280	2.79	550		1
		calc.	2.95	180	2.81	580	73.6	
^{11}B-^{11}C	$\frac{3}{2}^-$	expt.	0		0			14
		calc.	0		+0.08		59.7	
	$\frac{1}{2}^-$	expt.	2.12		2.00			
		calc.	2.12		2.15		55.9	
	$\frac{1}{2}^+$	expt.	6.79		6.34			
		calc.	6.77		6.35		79.3	
	$\frac{5}{2}^+$	expt.	7.29		6.91			
		calc.	7.19		6.97		81.7	
^{13}C-^{13}N	$\frac{1}{2}^-$	expt.	0		0			19
		calc.	0		−0.07		39.6	
	$\frac{1}{2}^+$	expt.	3.09		2.37	33		
		calc.	3.35		2.37	25	57.3	
	$\frac{5}{2}^+$	expt.	3.85		3.55	47		
		calc.	3.85		3.44	47	61.6	
^{15}N-^{15}O	$\frac{1}{2}^-$	expt.	0		0			19
		calc.	0		0.15		50.7	
	$\frac{5}{2}^+$	expt.	5.27		5.24			
		calc.	5.27		5.14		69.9	
	$\frac{1}{2}^+$	expt.	5.30		5.18			
		calc.	5.31		4.98		69.3	
^{17}O-^{17}F	$\frac{5}{2}^+$	expt.	0		0			19
		calc.	0		+0.025		57.4	
	$\frac{1}{2}^+$	expt.	0.87		0.495			
		calc.	0.87		0.40		53.8	
	$\frac{3}{2}^+$	expt.	5.09	96	5.10	1530		
		calc.	5.10	120	4.63	1200	45.0	
	$\langle\frac{3}{2}^+\rangle$[a]	expt.	5.87		5.60			
		calc.	5.86	480	5.50	1720	42.5	

[a]Centroids.

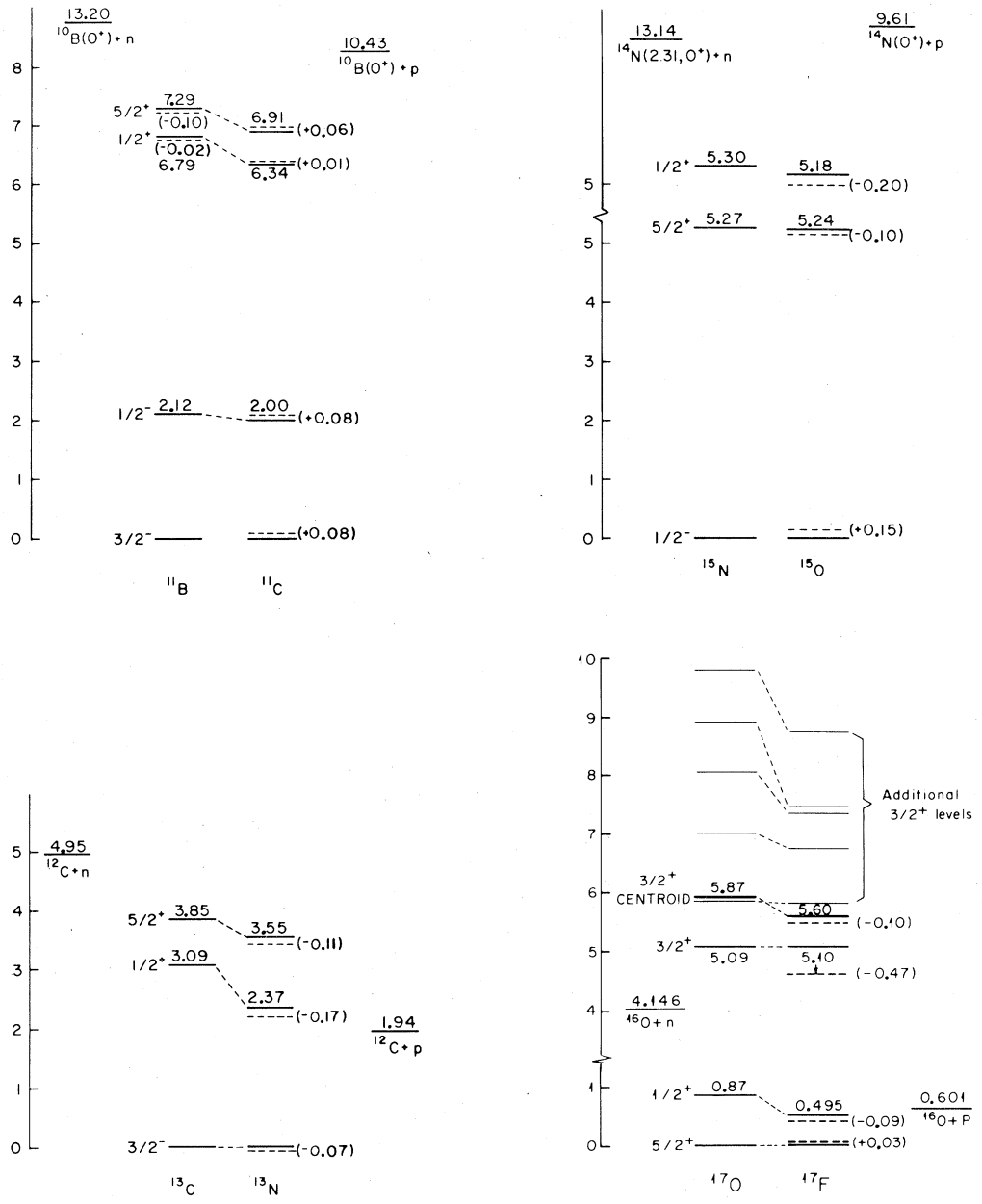

FIG. 1. Energy level diagrams for mirror states in $A=11$, 13, 15, and 17. Only the levels having predominant single-particle character are shown. For $A=17$, the lowest six $\frac{3}{2}^+$ states and their centroids are shown. Calculated values are displayed as dashed lines together with their displacement from the experimental values. (Energies are in MeV.)

mirror nuclei, both prescriptions give the same results within our desired accuracy. The resulting Coulomb displacement energies shown in Table II are consistently low, but no more than 260 keV. The very large shift of the $\frac{1}{2}^+$ state relative to the ground state (this is the famous case studied by Thomas and by Ehrman) is reproduced to within 190 keV. The widths of the unbound proton states are, of course, very sensitive to the energies. We therefore fit the potential to the proton-resonant energy rather than the neutron binding energy for this case. It may be seen from Table I that the widths agree quite well for both the $\frac{1}{2}^+$ and $\frac{5}{2}^+$ states, confirming their predominant single-particle character.

In the case of ^{17}O-^{17}F, the agreement is good for the bound $\frac{5}{2}^+$ and $\frac{1}{2}^+$ states. The only major failure of our model so far appears to be for the lowest $\frac{3}{2}^+$ resonances in this mirror pair: the calculated ^{17}F energy is 470 keV low. These states are high enough in the spectrum so that they mix significantly with other $\frac{3}{2}^+$ states. We find much better agreement between calculation and experi-

TABLE II. Coulomb displacement energies for the $1p_{3/2}$, $1p_{1/2}$, $2s_{1/2}$, $1d_{5/2}$, and $1d_{3/2}$ levels of Table I.

^{9}B-^{9}Be	J	$\frac{3}{2}^-$	$\frac{1}{2}^+$	$\frac{1}{2}^-$	$\frac{5}{2}^+$
	ΔE expt.	1.86	(1.8)	(1.7)	1.60
	ΔE calc.	1.76	1.16	1.47	1.72
^{11}C-^{11}B	J	$\frac{3}{2}^-$	$\frac{1}{2}^-$	$\frac{1}{2}^+$	$\frac{5}{2}^+$
	ΔE expt.	2.77	2.65	2.32	2.39
	ΔE calc.	2.85	2.79	2.35	2.55
^{13}N-^{13}C	J	$\frac{1}{2}^-$	$\frac{1}{2}^+$	$\frac{5}{2}^+$	
	ΔE expt.	3.01	2.28	2.69	
	ΔE calc.	2.94	2.02	2.58	
^{15}O-^{15}N	J	$\frac{1}{2}^-$	$\frac{1}{2}^+$	$\frac{5}{2}^+$	
	ΔE expt.	3.53	3.41	3.50	
	ΔE calc.	3.68	3.20	3.40	
^{17}F-^{17}O	J	$\frac{5}{2}^+$	$\frac{1}{2}^+$	$\frac{3}{2}^+$	$\langle\frac{3}{2}^+\rangle$
	ΔE expt.	3.55	3.18	3.56	3.25
	ΔE calc.	3.58	3.09	3.09	3.18

ment if we consider the reduced-width-weighted centroids as was done by Nolen and Schiffer[11] for the $2p_{3/2}$ states in $A=41$. The extra $\frac{3}{2}^+$, $T=\frac{1}{2}$ states[19] are shown in Fig. 1(d); their single particle strengths were measured in Refs. 18 and 21. The clumping near the lowest states (which have 69% and 51% of the Wigner limit, respectively) arises because the spin-orbit splitting is roughly the same as the excitation of particle-hole states.[20] The computed centroid for ^{17}O is 5.87 MeV, and that for ^{17}F is 5.60 MeV. Choosing V_0 to yield the experimental energy for ^{17}O, the computed energy for ^{17}F is within 0.1 MeV of the experimental centroid. While this is very satisfactory for the application of the potential model to single-particle shifts, we do not understand why there should be such large differences between ^{17}O and ^{17}F in the mixing with other states.

B. ^{9}Be and ^{9}B

We consider now our results for ^{9}Be and ^{9}B shown in Fig. 2 and Tables I and II. All the levels for both nuclei (excepting the ground state of Be) are particle unstable. Our computations take us into a new conceptual region of very broad states. Line shapes based on the probability of

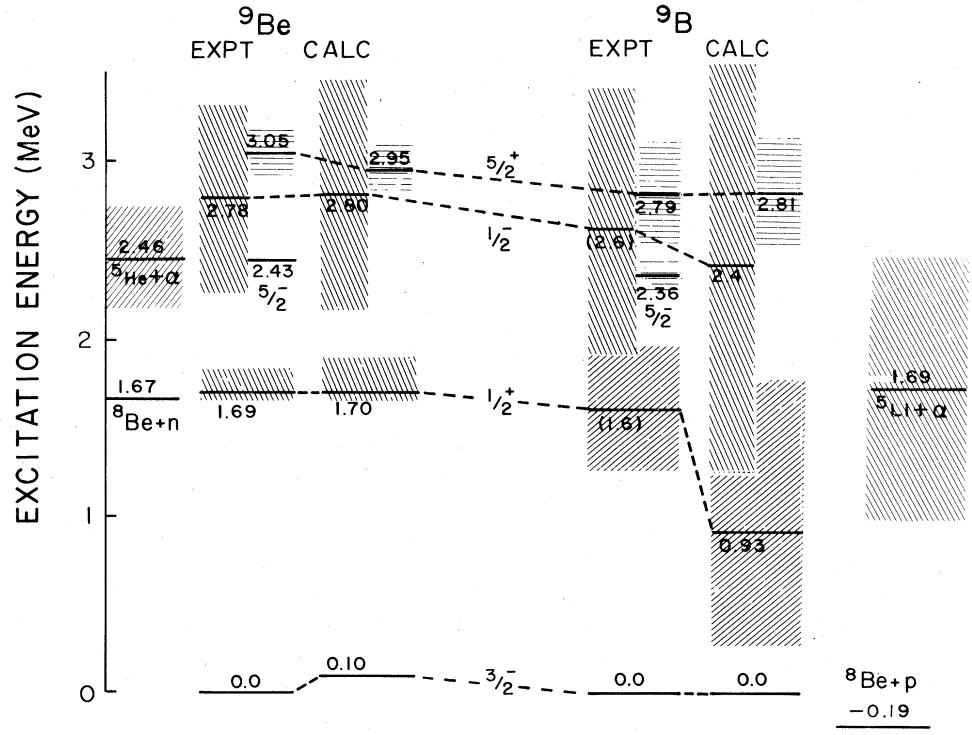

FIG. 2. Energy levels for ^{9}Be and ^{9}B. The experimental and computed values for each isotope are shown separately. The shaded areas indicate the FWHM for each level.

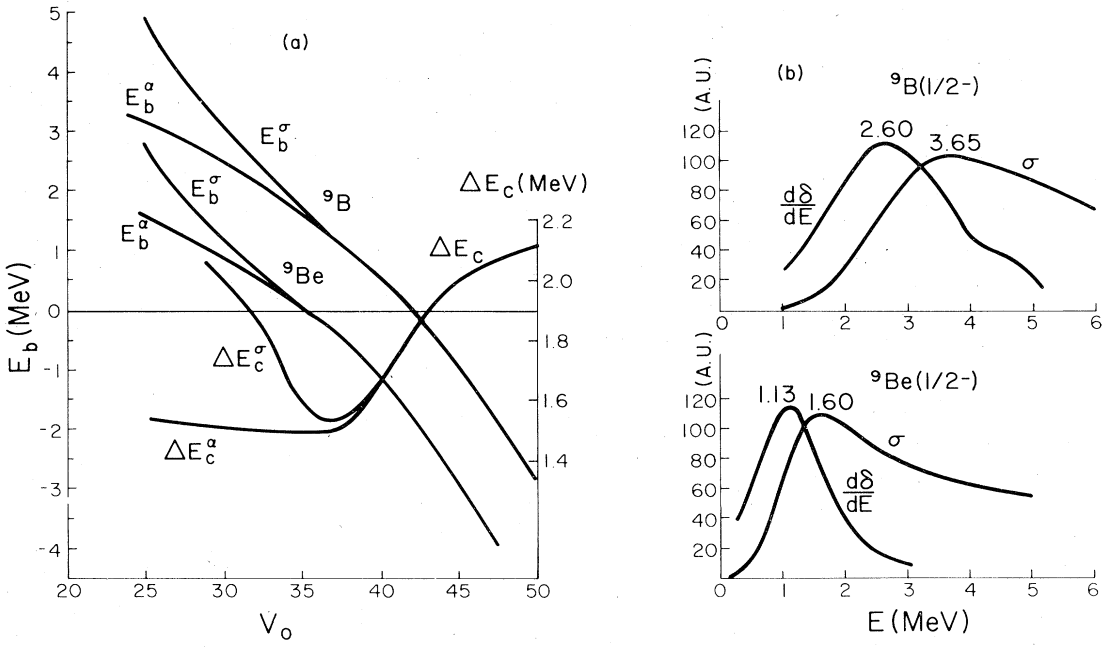

FIG. 3. (a) Calculated energies E_b (left scale) for the binding of the $1p_{1/2}$ neutron and proton in ^{9}Be and ^{9}B relative to ^{8}Be(0^+) as a function of potential well depth V_0. Also shown are the corresponding values of the Coulomb displacement energy ΔE_C (right scale). At low V_0, each curve divides into branches marked σ and α which are explained below and in the text. (b) Resonances for ^{9}Be and ^{9}B relative to the ^{8}Be core at 28.4 MeV. The curves marked σ are the probability [Eq. (2)] versus dissociation energy E, while those labeled $d\delta/dE$ or α are the derivatives of the phase shifts $d\delta/dE$ vs E.

the wave function in the nucleus for the $1p_{1/2}$ states are shown for $V_0=28.4$ MeV by the curves labeled "σ" in Fig. 3(b), and the dependence of the peak position E_b on potential well depth is shown in Fig. 3(a). As expected, the proton energy and the neutron energy increase as V_0 decreases. The Coulomb energy ΔE_C^σ (also shown) is just the difference between the two, and it decreases with decreasing V_0. All behavior is normal down to $V_0=38$ MeV. However, at lower V_0, ΔE_C^σ starts to increase. This unreasonable behavior begins when the scattering no longer displays a narrow, approximately symmetrical resonance shape. As seen in Fig. 3(b), the probability curves marked σ rise sharply with E, but fall off slowly. In these circumstances, the resonance energy can no longer simply be taken to correspond to the maximum of the probability. Instead, as noted earlier, we can use the energy corresponding to the maximum rate of change of scattering phase δ. The dependence of $d\delta/dE$ on E for $V_0=28.4$ MeV is shown in Fig. 3(b). The curves in Fig. 3(a) labeled by α show the dependence of the energy of the maxima of $d\delta/dE$ on potential well depth. With the $d\delta/dE$ prescription, the Coulomb displacement energy (designated by ΔE_C^α) behaves normally even well into the continuum. We therefore used the $d\delta/dE$ prescription for the energies and widths of the $1p_{1/2}$ and $1d_{5/2}$ states of $A=9$ listed in Table I.

We now consider the potential model description of the $2s_{1/2}$ states of ^{9}Be and ^{9}B. A major difficulty arises that was not encountered in the previous work;[11–15] namely, that for unbound $\frac{1}{2}^+$ levels, there is no potential barrier, and so the resonance does not exist in a rigorous sense. Therefore, we cannot compute the energy of the unbound $\frac{1}{2}^+$ state of ^{9}Be with either of the two resonance prescriptions. However, reactions do show a well-defined $\frac{1}{2}^+$ peak in the case of ^{9}Be, and we shall define the energy of the level to be the energy at which the following amplitude has a maximum:

$$C=\int \Psi_E(r) r \phi_0(r) r^2 dr \ , \tag{4}$$

where $\phi_0(r)$ is the bound state $1p_{3/2}$ wave function for the ^{9}Be ground state. The square of this amplitude is proportional to the probability of creating the continuum state from the ground state with the operator r, e.g., by a dipole transition in ^{9}Be. The line shape for this matrix element is compared in Fig. 4(a) for a potential well depth of 56.3 MeV with the reaction data[22] for ^{9}Be(γ,n)^{8}Be. The fit is only moderately good, and could not be improved over the wide range of measurement energy, no doubt due to the influence of other amplitudes besides the single-particle dipole matrix element. The R-matrix theory of Ref. 2 gives a better fit, but at the expense of introducing parameters which do not allow a prediction of the analog state energy. The shape of the cross section in the vicinity of

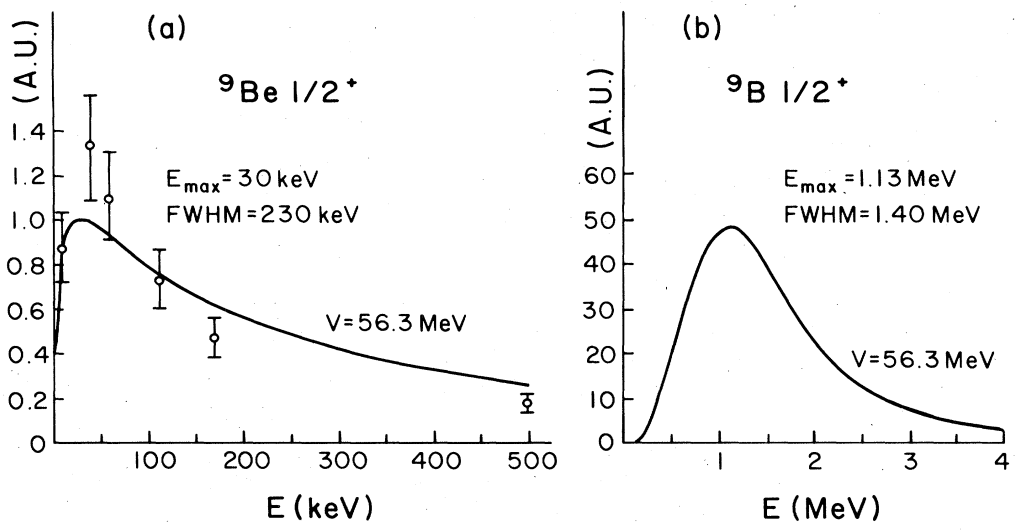

FIG. 4. (a) Line shape for the reaction ^{9}Be(γ,n)^{8}Be. The horizontal scale shows the energy in MeV above the ^{8}Be(0^+) + n threshold. Experimental data are from Ref. 22. The curve is the best fit prediction of the potential model [Eq. (4)] for V_0=56.3 MeV. (b) Predicted line shape for the excitation of ^{9}B($\frac{1}{2}^+$) from the ^{9}Be ground state. The energy scale is in MeV with respect to ^{8}Be(0^+) + ^{1}H.

the peak requires a well depth close to 56.3 MeV in the potential model. We use this value to predict the s-wave strength in ^{9}B.

Our calculated line shape for ^{9}B is shown in Fig. 4(b) for the same operator matrix element (4). Of course, there is no physical process that would produce such a matrix element; the closest is a charge exchange reaction which in the distorted wave Born approximation would have an integral such as Eq. (4) with the factor r replaced by a reaction form factor. The predicted $\frac{1}{2}^+$ strength in ^{9}B has a peak at 1.13 MeV, corresponding to an excitation energy of 0.93 MeV which is to be compared with E_x=1.68 MeV in ^{9}Be. Thus, the expected Thomas-Ehrman shift persists when the s-wave neutron also becomes unbound.

The experimental widths of the states in A=9 are quoted in Table I, and compared with our calculations. We have defined the width to be the full width at half maximum of the line shape. Of course, the shapes are quite asymmetric, so our widths do not necessarily have any relation to a true resonance width, which is twice the imaginary part of the pole position. The quoted experimental widths are reproduced better than might be expected considering the ambiguity in the choice of amplitude to measure. The deviation is, in all cases but one, on the side of too large a predicted width, which is consistent with the single particle model providing an upper bound on the widths.

III. SUMMARY

Our final result is the prediction that the $\frac{1}{2}^+$ state of ^{9}B is at an excitation energy of approximately 0.9 MeV, and has a width of about 1.4 MeV. The experimental and calculated energy levels for ^{9}Be and ^{9}B are summarized in Fig. 2. Also shown by the shaded areas are the widths of the states to emphasize one of the major difficulties in the experimental determination of these levels, namely the great degree of overlapping. Experiments to measure these levels have the severe additional problem of multiparticle final states which lead to large backgrounds above the ground states in all reactions.[3,7] To eliminate or minimize this background, one might carry out correlation experiments such as ^{9}Be(^{3}He,t) with coincidences between tritons and ^{8}Be alpha particle pairs from the breakup of ^{9}B measured at angles appropriate to a two-body final state. The precise shape of the ^{9}B spectrum remains, of course, to be calculated with a more detailed DWBA description; it will probably be broader than Fig. 4(b) and possibly angle dependent. A characteristic signature of the s-wave strength function would be the isotropic decay in the ^{9}B c.m. system, which could be reconstructed if the triton and the two alpha particles from the ^{8}Be were detected.

This work was supported by the National Science Foundation and the Department of Energy.

*Present address: Department of Physics and Astronomy and National Superconducting Cyclotron Laboratory, Michigan State University, East Lansing, MI 48824.

[1]F. Ajzenberg-Selove, Nucl. Phys. **A413**, 1 (1984).
[2]F. C. Barker, Can. J. Phys. **61**, 1371 (1983).
[3]R. W. Bauer, J. D. Anderson, and C. Wong, Nucl. Phys. **56**, 117 (1964).
[4]E. F. Farrow and H. J. Hay, Phys. Lett. **11**, 50 (1964).

[5]L. G. Earwaker, J. G. Jenkin, and E. W. Titterton, Nucl. Phys. **46**, 540 (1963); J. J. Kroepfl and C. P. Browne, *ibid.* **A108**, 289 (1968).
[6]K. Gul, B. H. Armitage, and B. W. Hooton, Nucl. Phys. **A153**, 390 (1970).
[7]H. Ueno, T. Nakagawa, M. Baba, J. Kasagi, H. Orihara, and T. Tohei, J. Phys. Soc. Jpn. **40**, 1537 (1976).
[8]A. Djaloeis, J. Bojowald, G. Paic, and B. Antolkovic, Kernforschungsanlage Jülich GmbH Institut fur Kernphysik, Annual Report, 1983, p. 11.; *Proceedings of the International Conference on Nuclear Physics, Florence, 1983* (Tipographia Compositori, Bologna, 1983), Vol. 1, p. 235.
[9]F. C. Barker and P. B. Treacy, Nucl. Phys. **38**, 33 (1962).
[10]R. R. Spencer, G. C. Phillips, and T. E. Young, Nucl. Phys. **21**, 310 (1960).
[11]J. A. Nolen, Jr. and J. P. Schiffer, Annu. Rev. Nucl. Sci. **19**, 471 (1968).
[12]K. Jones *et al.*, Phys. Rev. **145**, 894 (1966).
[13]J. A. Nolen, Jr. *et al.*, Phys. Rev. Lett. **18**, 1140 (1967).
[14]J. P. Schiffer, Nucl. Phys. **46**, 246 (1963).
[15]T. A. Tombrello, Phys. Lett. **23**, 134 (1966).
[16]W. Benenson *et al.*, Phys. Rev. C **9**, 2130 (1974); **15**, 1187 (1977); **17**, 1939 (1978).
[17]G. C. Phillips, T. A. Griffy, and L. C. Biedenharn, Nucl. Phys. **21**, 327 (1960).
[18]C. H. Johnson, Phys. Rev. C **7**, 561 (1973).
[19]F. Ajzenberg-Selove, Nucl. Phys. **A360**, 1 (1981); **A375**, 1 (1982).
[20]A. M. Bernstein, Ann. Phys. (N.Y.) **69**, 19 (1972).
[21]S. R. Salisbury and H. T. Richards, Phys. Rev. **126**, 2143 (1962).
[22]M. Fugishiro *et al.*, Can. J. Phys. **60**, 1672 (1982).
[23]A. Fazely *et al.*, Indiana University Cyclotron Facility Scientific and Technical Report, 1982, p. 49.